

## POST-IMPACT FIRE RESISTANCE OF T-STUB JOINT COMPONENT Numerical Evaluation

JoãoRibeiro <sup>a</sup>, Aldina Santiago <sup>a</sup>, Constança Rigueiro <sup>b</sup>

<sup>a</sup> ISISE, Faculdade de Ciências e Tecnologia, Universidade de Coimbra, Coimbra, Portugal

<sup>b</sup> ISISE, Escola Superior de Castelo Branco, Instituto Superior de Castelo Branco, Castelo Branco, Portugal

### Abstract

Current paper presents a finite element analyses for the characterization of the nonlinear behaviour of bolted t-stub component subject to impact loading followed by fire. The proposed numerical model has previously validated against experimental results under monotonic static loading at ambient and elevated temperatures (Ribeiro *et al.*, 2013). 3D solid and contact elements from the finite element package Abaqus are used to perform the structural model. The temperature dependent material properties, the geometrical and material nonlinearities (including the strain rate sensitivity) were taken into account to predict the failure of the t-stub. A parametric study was conducted to provide insight into the overall behavior, namely their stiffness, resistance, ductility and failure modes due to the effects of dynamic loading followed by fire.

**Keywords:** steel structures, numerical simulation, impact loading, elevated temperatures, T-stub component

### INTRODUCTION

The growing interest in robust design is a consequence of several events that led to the collapse of structures, like for example, the World Trade Centre (WTC) in 2001. The WTC attack has highlighted troublesome weakness in design and construction technologies on structural steel connections which exhibited poor performance when subject to impact loads and fire. The vulnerability of steel connections under dynamic actions has been emphasized by many studies, although most of them were performed for the purpose of mitigating seismic risk (Ellingwood *et al.*, 2007 and Luu, 2009), and few information exists concerning the performance of steel connections under impulsive loads (Yim, 2009, Tyas *et al.*, 2010 and Chang *et al.*, 2011).

Connections performance is directly linked to the robustness of steel structures due to the influence of its ductility and rotation capacity. Currently, the design of steel joints is based on the “component method” established in the Eurocode 3, Part 1.8 (EN1993-1-8, 2005). This method requires the accurate characterization (stiffness, resistance and ductility) of each active component; the t-stub is one of the main components that assure the joint ductility due to its high deformation capacity. This paper intends to study fire and impact loading and apply them to a finite element model for the representation of the nonlinear behaviour of bolted t-stub component under such conditions. Focus is given on the effects of damage due to impact loading on the evolution of structural response.

### 1 STRAIN RATE EFFECT

Strain rate is the deformation, i.e. strain variation, that a material is subject per unit time,  $d\epsilon/dt$ . Most ductile materials have strength properties which are dependent of the loading speed; mild steel is known to have its flow stress affected. The effects of strain rate on steel strength are illustrated in Fig. 1. The results were obtained from compressive Split Hopkinson Pressure Bar test (SHPB) (Saraiva, 2012); it was observed that yield and ultimate strengths

increase beyond the results obtained with a static test, the rupture strain decreases and the elastic modulus remains indifferent to the loading rate.

Finite element models aiming to simulate the behaviour of structural elements when subject to impact loads require a constitutive law representing the behaviour of materials at high strain rates. Cowper-Symonds and the Johnson–Cook constitutive laws are the widely used in numerical simulations. In the current model, the strain rate effects were considered by the Johnson–Cook law, Eq. (1).

This law describes material hardening through an exponential function and is able to account for strain rate sensitivity and thermal softening behaviours. The constitutive law assumes that the slope of flow stress  $\sigma_y$ , is independently affected by each of the mentioned behaviours; therefore, only the second term (accounting for strain sensitivity) of the equation has been used.

$$\sigma_y = [A + B\varepsilon^n] \cdot [1 + C \ln \dot{\varepsilon}^*] \cdot [1 - (T^*)^m] \quad (1)$$

where:  $A$  is the yield stress;  $B$  and  $n$  represent the effects of strain hardening;  $m$  is the thermal softening fraction;  $\varepsilon$  is the equivalent plastic strain;  $\dot{\varepsilon}$  is the strain rate, and  $\dot{\varepsilon}^* = \dot{\varepsilon}/\dot{\varepsilon}_0$  is the dimensionless plastic strain rate for  $\dot{\varepsilon}_0 = 1.0 \text{ s}^{-1}$ ;  $C$  is the strain rate constant.

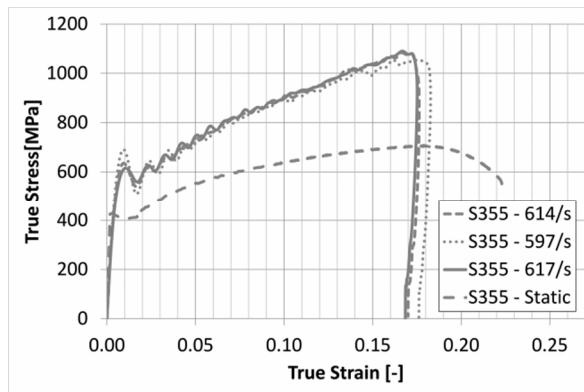


Fig. 1 Stress strain relationship of steel under high-strain rate (approx.  $600 \text{ s}^{-1}$ ) for  $t = 15 \text{ mm}$  plate, S355 (Saraiva, 2012)

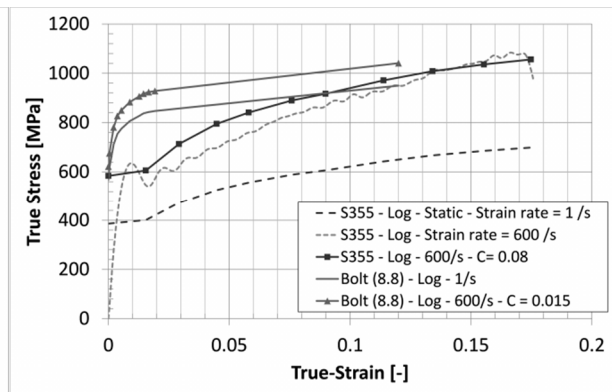


Fig. 2 Stress strain relationship for mild steel and bolts considering Johnson-Cook strain rate sensitivity

## 2 NUMERICAL MODEL

### 2.1 Description of the FE Model

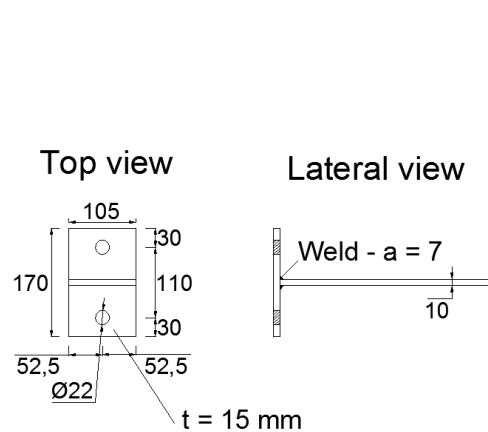


Fig. 3 T-stub geometry

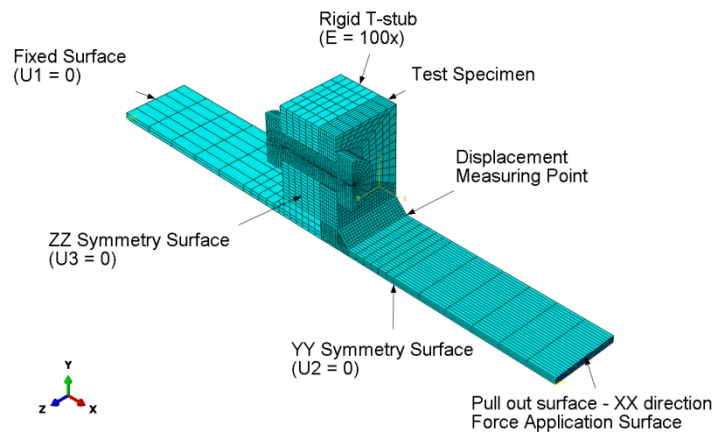


Fig. 4 Numerical model, boundary condition and mesh discretization

The numerical model is drawn from a previous study carried out at University of Coimbra, where numerical models under monotonic static loading at ambient and elevated temperatures (500 °C and 600 °C) were developed (Ribeiro *et al.*, 2013). Fig. 3 and Fig. 4 present the dimensions of the test specimens and the numerical model with boundary condition and mesh discretization. The flange was bolted through two bolts M20, grade 8.8 partially threaded.

The FE model is composed of four parts: (i) rigid back t-stub; (ii) tested t-stub; (iii) bolt, (head and shank as a single piece) and (iv) pull-out plate, as depicted in Fig. 4. Contact conditions are modelled between all the four parts namely: (i) the bottom flange surface with the back t-stub bottom flange; (ii) bolt shank with flanges bolt hole; (iii) top flange surfaces with bolt head; and (iv) pull out plate contact with the tested t-stub once the welds showed very little penetration. The welds have been modelled with tie constraint property linking the pull out plate to the tested t-stub part. Normal contact conditions are accomplished with “hard-contact” property allowing for separation after contact and the tangential behaviour has been assumed with a friction coefficient of 0.2 following “penalty” formulation. Bolt modelling followed the nominal geometry (bolt shank diameter with 20 mm). No pre-load has been considered.

The t-stub model has been simplified by the use of symmetry conditions in axes  $yy$  and  $zz$ ; therefore, displacements in these directions are restrained at the symmetry surfaces (Fig. 4). The model was generated with solid element type C3D8R, allowing large deformations and non-linear geometrical and material behaviour. C3D8R is a valuable choice due to its reduced integration (only 1 integration point) allowing for reductions in calculation time while it provides hour-glass behaviour control. Generally a structured mesh technique with “Hex” element shape is used, except for the weld zone where a “Wedge” element shape was employed.

Mesh discretization studies were previously conducted assuring that a discretization of at least 4 elements through the thickness of bending-dominated plates (t-stub flanges), and a concentric mesh around the bolt area provided accurate results, whilst optimizing calculation time and reducing convergence problems.

## 2.2 Material Properties

Material nonlinearity was included by specifying a non-linear stress-strain relationship for material hardening; Von Mises criterion was considered to establish the yield surfaces with the associated plastic flow for isotropic materials (Abaqus, 2006). Stress-strain relationship has been obtained through uniaxial coupon tests at ambient temperature (Santiago *et al.*, 2013). The mean results are: elastic modulus,  $E = 205500$  MPa, elastic strength,  $f_y = 385$  MPa; ultimate strength,  $f_u = 588$  MPa and ultimate strain,  $\epsilon_{cu} = 24\%$  for the steel. Uniaxial tension test on a M20 grade 8.8 bolt measured  $E = 202500$  MPa;  $f_y = 684$  MPa;  $f_u = 1002$  MPa and  $\epsilon_{cu} = 3.7\%$ . Once the bolt geometry follows nominal dimensions, bolt material properties have been revised to take into account the reduced tensile shank area. Material properties for the weld at ambient temperatures have been assumed equal to the base steel plates. For elevated temperature material models proper reduction factors reported in Eurocode 3, Part 1-2 (CEN, 2005) have been used for the mild steel, bolt, and also the weld. Once large strains and large displacements are expected, material’s constitutive law is included in the numerical model by the *true-stress – logarithmic plastic strain* curves (Fig. 2). As mentioned before, material strain rate sensitivity has been included using the second term of JC model.  $C_{steel} = 0.08$  for  $600\text{ s}^{-1}$  was calculated from data obtained from SHPB tests (Saraiva, 2012) (Fig. 2). The literature indicate that high strength steels are less sensible to the effects of strain rate variation; According Chang *et al.*(2011) a dynamic increase factor (DIF) of 1.1 may be considered for the bolts; moreover, impact tests on A 325 bolts recovered from the WTC debris showed very low sensitivity to strain rate (Ellingwood *et al.*, 2007). In the current study, a DIF = 1.1 has been considered for bolt grade 8.8 for a strain rate of  $600\text{ s}^{-1}$ , thus a value of  $C_{bolt}=0.015$  was adopted (Fig. 2). The welds were assumed to have the same strain rate sensitivity as the base steel.

The Johnson–Cook law provides strain rate hardening varying linearly with the logarithm of strain rate; thus from  $1\text{s}^{-1}$  to  $600\text{s}^{-1}$  further data is required in case a non-linear variation of the flow stress with strain rate occurs.

### 2.3 Failure criterion

Material damage properties proposed by Hooputra (2004) and Al-Thairy (2011) are assumed in the current study (Fig. 6). These values are based on calibration to the observed failure modes from t-stub static tests and ultimate strain measured in uniaxial tests and SHPB.

### 2.4 Impact and fire loading

The study of rapidly applied loading such as an impact requires a dynamic analysis, once inertia effects of the system can no longer be disregarded; static force equilibrium is not required to be fulfilled. In order to take geometric non-linearities, material plasticity and strain rate behaviour into account, a non-linear dynamic analysis must be put through. In the proposed study the Abaqus dynamic/implicit solver is used.

The numerical analysis is divided in two steps: first, the impact loading is applied using a linear increasing load in 20 milliseconds (from zero to maximum load magnitude); a parametric study of the maximum load ranging from 200 to 900 kN is made. After the impact load reaches the maximum value, the load is decreased to zero in 5 milliseconds; then t-stub is left to vibrate during another 5 milliseconds. Afterwards a static load with magnitude of 70% of the analytical design resistance is set and a linear increase of temperature is applied.

## 3 ANALYSIS RESULT OF T-STUB SUBJECT TO IMPACT AND FIRE

### 3.1 Validation of the numerical model against experimental results under monotonic loading

Fig. 5 compares the numerical predictions (dashed lines) with the experimental results (solid lines) at ambient temperature and elevated temperatures of the t-stub component subject to monotonic static loading. It can be observed that the numerical model can accurately predict the global behaviour of the t-stub component. Considering the failure criteria exposed above, bolt rupture is the ultimate numerical failure mode for all numerical analysis; failure is identified with diamond marker in Fig. 5. Tests at ambient temperature exhibited bolt rupture at 14 mm of web displacement; test at 500 °C exhibited flange cracking around 10 mm of web displacement while for the 600 °C a long horizontal plateau is developed due to long bolt elongation.

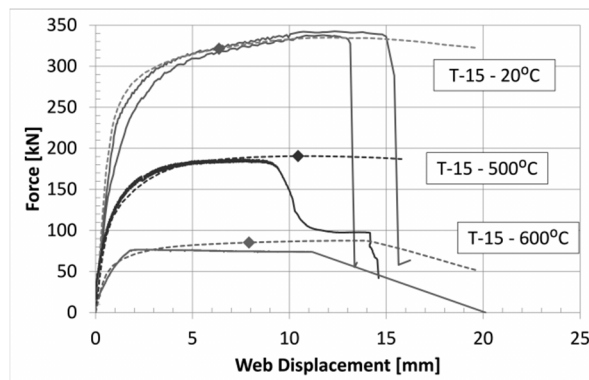


Fig. 5 Response of t-stub at 20, 500 and 600 °C: numerical versus experimental results (Ribeiro *et al.*, 2013)

### 3.2 T-stub subject to impact and fire

For the analysis at elevated temperatures, it has been assumed: (i) temperature variation introduced as a pre-defined field; (ii) high temperature creep effects of steel have not been taken into account; (iii) the temperature has been assumed to be constant throughout the FE model; and (iv) expansion effects due to temperature increase according to EC3 Part. 1-2 (CEN, 2005).

Fig. 7 illustrates the numerical predictions of the t-stub response under the impact loads; comparison with static test can also be made; it can be observed that with the increase of impact loading: i) that the elastic stiffness is not affected, as the elastic modulus remains unchanged; and ii) transition knee caused by the plastic hinge in the t-stub flange is similar for different impact loads; iii) the strain rate variability within the applied force range is very low; also, iv) compared with the static response the force at which the plastic hinge is formed is increased by +8%, far below the  $f_{y,din}/f_y = +51%$  obtained from coupon tests comparison, Fig. 2. This is because the flange is not subject to a strain rate of  $600 \text{ s}^{-1}$  but mostly below  $80 \text{ s}^{-1}$ , as presented for the 900 kN load case (Fig. 8). For loads over 375 kN the t-stub failed under impact load; Fig. 9 presents results for impact load range of 300 to 375 kN: a critical temperature of  $560 \text{ }^\circ\text{C}$  is predicted for all models with failure due to bolt rupture. Within this study, it was observed, that the impact load imposes damage in the flange next to the weld toe, but not in the bolt; thus, the bolt failure at elevated temperature is not conditioned by previous impact load and all models fail with the same critical temperature. T-stubs subject to lower impact loads exhibit longer displacement development capacity when subject to temperature increase.

		Johnson-Cook		Bolt		Weld		Steel	
		C=		0.015		0.08		0.08	
		Strain-rate		600		600		600	
Ductile Dam.	Fracture strain	0.3	0.3	-	-	0.2	0.16		
	StressTriaxiality	0.7	0.7	-	-	0.7	0.7		
	Strain Rate	1	600	-	-	1	600		
	Evolution	0.1		-	-	1			
Shear Dam.	ks	0.3	0.3	0.3	0.3	0.3	0.3		
	Fracture Strain	0.3	0.3	0.1	0.1	0.1	0.1		
	Shear Stress Ratio	0.7	0.7	0.7	0.7	0.7	0.7		
	Strain Rate	1	600	1	600	1	600		
	Evolution	0.01		1		1			

Fig. 6 Material damage parameters

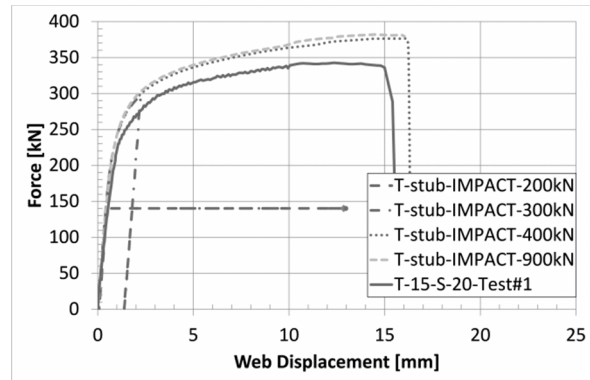


Fig. 7 T-stub response

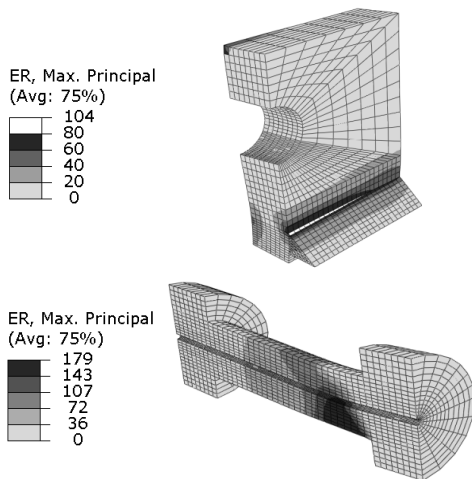


Fig. 8 Strain rate pattern for load of 900 kN

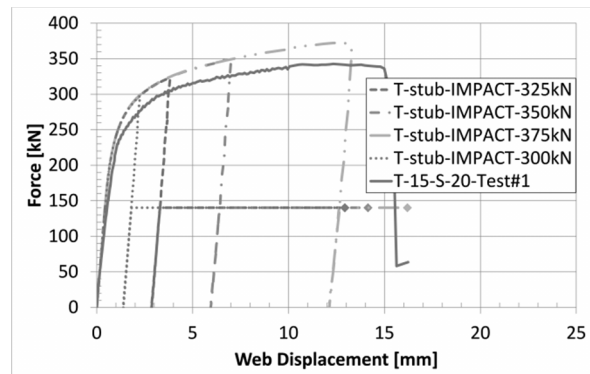


Fig. 9 T-stub response –  $\theta_{crit} = 560 \text{ }^\circ\text{C}$

## 4 SUMMARY

A FE model calibrated to static tests at ambient and elevated temperatures is enhanced to capture the behaviour of the t-stub component subject to several impact load levels, ranging from 200 to 900 kN in 20 milliseconds. Afterwards, the damaged t-stub is subject to a static load equivalent to 70% of the analytical design resistance and the temperature is increased up to failure; predictions of the critical temperature are made. Temperature material softening considers EC3 Part 1.2 (CEN, 2005) reduction factors. Strain rate effects have been taken into account with the Johnson-Cook strain sensitive term calibrated to compressive Split Hopkinson Pressure Bar tests at a strain rate of  $600\text{s}^{-1}$ . Although damage material properties are calibrated to fit observed failure modes from static t-stub tests and static uniaxial tension tests, both ambient and elevated temperatures, there are still great reservations in assessing the damage parameters, especially for high strain rates.

Taking into account the assumed failure criterion, the t-stub is able to resist a maximum impact load of around 375 kN. If the impact load does not damage the bolt, its fire resistance is not affected. Although they exhibit the same critical temperature, those subject to lower impact loads are able to develop longer displacement variation when subject to elevated temperatures; even if the absolute failure displacement is smaller.

## 5 ACKNOWLEDGMENT

The authors acknowledge financial support from Ministério da Educação e da Ciência (Fundação para a Ciência e a Tecnologia) under research project *PTDC/ECM/110807/2009*.

## REFERENCES

- Ellingwood, B.R., et al., Best Practices for Reducing the Potential for Progressive Collapse in Buildings 2007: NISTIR 7396.
- Luu Nguyen Nam, H. Structural response of steel and composite building frames further to an impact leading to the loss of a column. 2009.
- Yim, H.C. and Krauthammer, T., "Load-impulse characterization for steel connections", International Journal of Impact Engineering, Vol. 36, No. 5, pp. 737-745, 2009.
- Tyas, A., Warrem, J. A., Davison J.B., Stoddart E.P., and Hindle, A., Dynamic tests of semi-rigid beam-column connections in Proceedings of the COSTC26 International Conference on Urban Habitat Constructions under Catastrophic Events, Naples 2010.
- Chang, L., Hai, T., Ching, F., Tyas, A., "Numerical simulation of steel bolted beam-column connections subject to dynamic loading" Journal of Applied Mechanics and Materials, 2011.
- CEN, Eurocode 3: Design of steel structures part 1-8: Design of joints, 2005, Brussels: European Committee for Standardization.
- Saraiva, E., Variação das propriedades mecânicas do aço relacionadas com problemas de impacto em estruturas, in portuguese, Master Thesis at University of Coimbra, 2012.
- Barata P., Rigueiro M.C., Santiago A. e Rodrigues J.P., "Characterization of impact scenarios in steel structures"; pp. 242-249, Proceedings of the IABSE Workshop on Safety, Failures and Robustness of Large Structures, Helsinki, Finland, February 2013.
- Ribeiro J. N., Rigueiro C., Santiago A., Numerical behaviour of t-stub joint component at ambient and elevated temperatures, in 2° CISLACI 2013: Coimbra (paper submitted).
- Abaqus, "ABAQUS analysis: user's manual 2006", Providence, RI: ABAQUS Inc.
- Santiago A., Martins D., Barata P. e Jordão S., "Propriedades mecânicas do aço a temperaturas elevadas"; 2° CILASCI - Congresso Ibero-Latino-Americano sobre Segurança contra Incêndio, Coimbra, Portugal, June 2013

- CEN, "Eurocode 3: Design of steel structures. Part 1-2, General rules - Structural fire design", 2005, Brussels: European Committee for Standardization.
- Seidt, J.D., Gilat, A., Klein, J.A., Leach, J.R., "High Strain Rate, High Temperature Constitutive and Failure Models for EOD Impact Scenarios", Proceedings of the 2007 SEM Annual Conference and Exposition on Experimental and Applied Mechanics, Springfield, MA, June, 2007
- CEN, "Eurocode 3: Design of steel structures. Part 1-2, General rules - Structural fire design", 2005, Brussels: European Committee for Standardization.
- Hooputra, H., H. Gese, H. Dell, and H. Werner, "A Comprehensive Failure Model for Crashworthiness Simulation of Aluminium Extrusions," International Journal of Crashworthiness, vol. 9, no.5, pp. 449-464, 2004
- Al-Thairy, H., Wang, Y.C., "A numerical study of the behaviour and failure modes of axially compressed steel columns subjected to transverse impact", International Journal of Impact Engineering, vol. 38, pp. 732-744, 2011